Electronic Journal of Biotechnology 71 (2024) 28–36

Contents lists available at ScienceDirect

Electronic Journal of Biotechnology

journal homepage: www.elsevier.com/locate/ejbt

Research article

Virtual screening and experimental analysis of caspase-7 inhibitors as candidates for extending the lifespan of CHO cells ☆

Sara Kafi [a], Sajad Najafi [b,c], Karim Mahnam [d], Shirin Farivar [a,*], Javad Ranjbari [b,c,*]

[a] Department of Cell and Molecular Biology, Faculty of Life Sciences and Technology, Shahid Beheshti University, Tehran, Iran
[b] Pharmaceutical Sciences Research Center, Shahid Beheshti University of Medical Sciences, Tehran, Iran
[c] Department of Medical Biotechnology, School of Advanced Technologies in Medicine, Shahid Beheshti University of Medical Sciences, Tehran, Iran
[d] Department of Biology, School of Sciences, Shahrekord University, Shahrekord, Iran

GRAPHICAL ABSTRACT

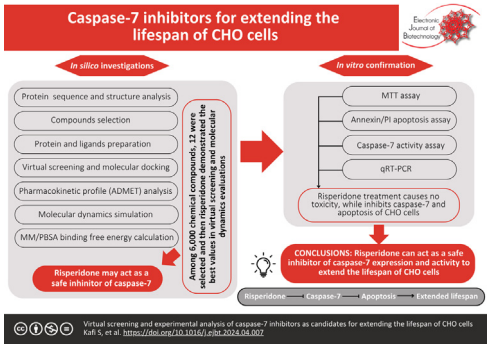

ARTICLE INFO

Article history:
Received 13 December 2023
Accepted 29 April 2024
Available online 13 June 2024

Keywords:
Anti-apoptotic
Apoptosis inhibition
Caspase-7
Caspase-7 inhibitors
CHO cells
Lifespan
Recombinant proteins
Risperidone
Virtual screening

ABSTRACT

Background: Chinese hamster ovarian (CHO) cells are widely employed in biotechnology for the production of recombinant proteins. Extending the life span of CHO cells and inhibiting the loss of producing cell population through the inhibition of apoptosis can benefit the productivity of those cells. In this study, we aimed to screen and evaluate the impact of some caspase-7 inhibitor candidates on the lifespan of CHO cells.

Results: Through virtual screening and molecular docking, risperidone was screened and selected as a potential inhibitor of caspase-7 in CHO cells. The results of MTT assay revealed that the cytotoxicity of risperidone at all concentrations was lower than 50%, and thus it can be suggested as a safe treatment for CHO cells. Annexin V apoptosis and flow cytometry assays revealed that risperidone at 1, 25, and 50 μM concentrations inhibited apoptosis 72 h post-treatment through caspase-7 inhibition. Although gene expression analysis through qRT-PCR demonstrates that risperidone did not affect caspase-7 gene expression.

Conclusions: This bioinformatics and experimental study suggests risperidone as a caspase-7 inhibitor with the potential to extend the lifespan of CHO cells and offers possible opportunities in biotechnology.

How to cite: Kafi S, Najafi S, Mahnam K, et al. Virtual screening and experimental analysis of caspase-7 inhibitors as candidates for extending the lifespan of CHO cells. Electron J Biotechnol 2024;71. https://doi.org/10.1016/j.ejbt.2024.04.007.

☆ Audio abstract available in Supplementary material.

Peer review under responsibility of Pontificia Universidad Católica de Valparaíso

* Corresponding authors.
E-mail addresses: s_farivar@sbu.ac.ir (S. Farivar), javadr63@gmail.com (J. Ranjbari).

https://doi.org/10.1016/j.ejbt.2024.04.007

1. Introduction

Recombinant therapeutic protein technology has served as one of the most valuable achievements in biomedical biotechnology and has changed modern medicine during the past decades [1,2]. Production of recombinant proteins for therapeutic targets at high levels in engineered organisms has been successfully employed as an alternative for the extraction of those vital elements from natural sources [3]. Additionally, recombinant production shows advantages including lower expenses, more extensive sources, higher concentrations, and less possibility of contamination compared to natural extraction methods [4]. Based on the protein's complexity of structure, feasibility of scale-up, costs, and type of use, several kinds of engineered hosts, including bacteria, yeasts, as well as plant, insect, and mammalian cells are being employed for the production of recombinant proteins [5].

Among eukaryotic cells, which show good features required for the function of engineered proteins like posttranslational glycosylation modification, Chinese hamster ovary (CHO) cells are being used for the production of approximately 70% of therapeutic proteins and the annual market of CHO products reaches 30 billion dollars globally [6]. CHO cells grow in both suspended and attached forms, can easily receive the foreign DNA for engineering purposes, generate the protein of interest in large quantities and glycosylated form with easy scale-up, while not releasing toxic elements into the environment and some pathogenic viruses cannot contaminate CHO cells [3,7]. Apoptosis is a physiological form of programmed cell death (PCD), which is a major problem during the production of biopharmaceuticals, such as recombinant proteins in animal cell hosts [8]. Extending the life span of CHO cells *in vitro* and avoiding the loss of the producing cell population through inhibition of apoptosis is one of the potential approaches for improving those cells' productivity.

Caspases are a group of cysteine proteases-peptidases recognized as the main effectors of apoptosis [9]. Numerous caspases are proteolytically activated in a cascade of events, eventually leading to phenotypic and structural changes of apoptosis and the demise of the cell [10]. Two intrinsic and extrinsic pathways of apoptosis employ two classes of caspases: initiator (caspases-8, and −9), and executioner (caspases-3,-6, and −7) [11]. Caspase-7 is a 34 kDa protein composed of 303 amino acids with α-helices and β-sheet structure, which shares several features like function with another executioner caspase-3, and when cleaved and activated (by the effector caspase-1) results in several morphological and biochemical apoptosis hallmarks like DNA fragmentation and nuclear condensation [10,12]. Inhibition of caspase-7 is suggested as a therapeutic approach for neurodegenerative diseases, ischemia, and sepsis [12]. We already have virtually screened the potential inhibitors of caspase-3 as therapeutic candidates for traumatic brain injury (TBI) [13], and in the current study, we investigated the inhibitory effect of some Iranian herbals, FDA-approved, world-not-FDA approved and investigational compounds on caspase-7, using protein–ligand docking method and then evaluate the impact of selected caspase-7 inhibitors on the gene expression and activity of caspase-7 enzyme in CHO-K1 cells.

2. Methods

2.1. Protein sequence and structure analysis

Human caspase-7 protein (UniProtKB: LocusCASP7_HUMAN, Accession No. P55210) (https://www.uniprot.org/) contains 303 amino acids weighting 34 kDa, and its encoding gene is located on chromosome 10. Caspase-7 is an effector enzyme that is activated by the catalytic activity of caspase-1 [10]. In the active site, caspase-7 possesses a catalytic cysteine residue responsible for the cleavage of target proteins [14]. The procaspase-7 is a homodimer composed of a 12-stranded β-sheet besieged by 10 α-helices [15]. This fold contains two enzymatic units with two distinct active sites [12]. Two small and large subunits are connected by a linker that is removed upon activation by the initiator caspase [16].

2.2. Compound selection

In the first step, by searching the literature, 59 native Iranian herbals with confirmed anti-inflammatory and anti-apoptotic roles were selected. The active ingredients of those herbals were researched for in the literature and eventually, a total number of 400 compounds were screened for the study. The three-dimensional (3D) structure of all compounds was retrieved from the PubChem BioAssay database (available at: https://pubchem.ncbi.nlm.nih.gov/) and saved as Simulation Description Format (SDF) files. Then, using the ZINC15 database (https://zinc15.docking.org/) [17], 1379 compounds with Food and Drug Administration (FDA) approval, 2068 non-FDA-globally approved compounds, and 2368 investigational compounds were retrieved in SDF files and used as ligands for molecular docking. The crystal structure of the human unliganded caspase-7 protein (Accession No. 3IBF, PDB https://doi.org/10.2210/pdb3IBF/pdb) was retrieved from the RCSB Protein Data Bank (RCSB PDB) (https://www.rcsb.org/), and then water molecules were removed from the structure using the Chimera software [18].

2.3. Protein and ligand preparation

The human caspase-7 was used as the receptor in the analyses, in which its unliganded crystal structure was retrieved from the RCSB protein data bank (PDB ID: 3IBF) (https://www.rcsb.org/). Chimera was used for removing the H_2O molecules from the structure. Conversion of the ligand SDF files into mol2 format was conducted using the Open Babel toolbox [19]. Then, the format of ligands was converted into PDBQT files using raccoon software [20].

2.4. Structure-based virtual screening, molecular docking

Using AutoDock Vina 1.2.0 software [21], molecular docking of the ligand–protein complex on input PDBQT files was conducted to determine the potential ligand–protein interactions and estimate the binding affinity of ligands (setting: exhaustiveness: 8, grid box with centers x: 20.7, y: −4.7, and z: 7.2 and grid dimension: 30 × 27 × 27 points). Those compounds with the binding affinity value <−8Kcal were selected for further analyses. To visualize and analyze the docking output, PyMOL and the Biovia Discovery Studio Visualizer 2020 [22,23] were employed. Considering several parameters, such as bonding energy and interaction patterns, 100 compounds with the best values were selected for the absorption, distribution, metabolism, excretion, and toxicity (ADMET) studies.

2.5. Pharmacokinetic profile analysis and binding interaction

The ADMET profiles of the 100 selected compounds were analyzed using admetSAR and SwissADME free web tools [24,25]. To identify the substantial parameters required for the analysis of medicine candidates, Lipinski's rule of five was used. These rules are employed for the initial quick evaluation of compounds in drug discovery and optimization processes that mainly focus on the solubility and permeability profiles of candidates. The SwissADME web tool (available at: https://www.swissadme.ch) was used for the estimation of the physicochemical properties of compounds [25]. A total of 43 compounds that followed those rules showed the proper drug-likeness criteria and thus, were selected for further analyses.

2.6. Molecular dynamics simulation

Using PyMOL software, complexes of caspase-7 and those 43 selected compounds were created and then evaluated using the Discovery Studio software. Eventually, 12 ligands with the most potent and abundant bonds were selected for molecular dynamics simulation. The molecular dynamics (MD) simulations of all 12 complexes retrieved from the previous screening and the unliganded caspase-7 were conducted *via* the Gromacs 5 under the G43A1 force field [26]. The complexes were placed in the center of a cubic box occupied by 12,330 SPC216 water models located with a 1 nm space from the edges. For simulation of the physiologic condition, an ionic strength of 0.14 M was applied. The energy levels were minimized and equilibrated. Eventually, an isothermal coupling ensemble (NPT) was employed to generate MD simulations at 310 K considering a time step of 0.002 ps. In the end, after calculating the average 17 binding free energies of the ligands, those compounds with the best free binding energy were selected for the next investigations. Protein-ligand complexes were also evaluated by importing to the DS visualizer 2.0, Accelrys Inc. for screening the interactions with the most potent bonds.

2.7. MM/PBSA binding free energy calculation

The G_mmpbsa module was used for the molecular mechanics Poisson-Boltzmann surface area (MM/PBSA) calculations and prediction of the protein–ligand binding free energy [27,28]. The Gromacs 5 was employed for the computation of molecular mechanical energy (E_{MM}), and polar and non-polar bond energies (G_{polar} and $G_{non\text{-}polar}$). For each complex, these measures were computed for 17 snapshots recorded in 300 ps intervals from the production trajectories during the final 5 ns of MD simulations.

2.8. In vitro experiments

2.8.1. Cell culture and reagents

CHO-K1 cells were purchased from the Pasteur Institute of Iran, and cultivated in a T-25 flask with 5 ml of DMEM-F12 medium supplemented with 10% fetal bovine serum (FBS, Gibco) in addition to 1% penicillin–streptomycin antibiotics, and incubated at 37°C humid incubator with 5% CO_2. By reaching 90% confluence, cells were washed with 3–5 ml phosphate-buffered saline (PBS), digested with 0.25% trypsin-EDTA (Gibco), incubated at 37°C for 5 min, and then, 10% FBS-supplemented DMEM-F12 was added to the cell concentrate to stop the digestion. For cell subculture, the suspended cells were collected in a 15 ml tube and centrifuged at 1500 rpm for 5 min and then, 1% of the pellet volume was added to 5 ml of FBS-supplemented DMEM-F12 in a T-25 flask.

2.8.2. MTT assay

To assess the toxicity of risperidone on survival and proliferation of CHO-K1 cells, the 3-(4, 5-dimethylthiazol-2-yl)-2, 5-diphenyltetrazolium bromide (MTT) reduction assay was employed according to the manufacturer's instructions (Sigma-Aldrich). A population of 30,000 cells were seeded and treated with three certain concentrations of risperidone (100 nM, 20 μM, and 100 μM). Each plate was treated with a 100 μM volume of MTT at 1 M concentration, covered with aluminum foil and incubated at 37°C for 3–4 h. The MTT indicator was removed and 100 μL of the solvent was added to solve formazan crystals. The absorbance of the plates was read by a spectrophotometer at 570 nm. The toxicity was calculated using the formula:

$$Cytotoxicity(\%) = \frac{(Sampleabsorbance - Backgroundabsorbance)}{(Controlabsorbance - Backgroundabsorbance)} \times 100$$

2.8.3. Annexin/PI apoptosis assay

Annexin/PI apoptosis assay was conducted to evaluate the impact of risperidone on the apoptosis of CHO-K1 cells. Annexin/PI apoptosis assessment kit (Anacell, Iran) was used according to the manufacturer's instructions. Briefly, CHO-K1 cells were seeded at a total count of 1,200,000 per each well. However, 24 h later, the cells were attached to the plate and then treated with risperidone at concentrations of 1, 25, and 50 μM. Post-treatment evaluation of annexin-V was conducted in 24, 48, and 72 h. To prepare the cells for evaluating annexin-V, cells were washed with 500 μL of PBS, digested using 500 μL of trypsin, and then, the centrifuged pellet was resuspended in 90 μL of diluted annexin-V solution. A total of 5 μL of conjugated annexin-V and 5 μL of propidium iodide were added to each well and incubated in darkness for 20 min. Four hundred μL of annexin-V solution was added to the cell suspension and centrifuged at 400 rpm for 5 min; then, the cell pellet was resuspended with 400 μL annexin-V solution and analyzed by flow cytometry.

2.9. Evaluation of caspase-7 activity

Caspase-7 activity kit (Kiazist, Iran) was used for *in vitro* assessment of caspase-7 activity. According to the manufacturer's instructions, 1,200,000 CHO-K1 cells were seeded in each well and treated with risperidone at 1, 25, and 50 μM and then, caspase-7 activity was evaluated 24, 48, and 72 h post-treatment. Cells were trypsin-digested, and centrifuged, and then, the pellet was resuspended in 500 μL of caspase lysis buffer and incubated at 4°C for 20 min to lyse the cells. The cell lysate was centrifuged at 12,000 rpm for 15 min at 4°C. 50 μL of cell lysate in addition to standard and positive controls was added to each 96-well plate. 5.55 μL of the working solution (caspase buffer

Table 1
A list of 12 compounds with the highest affinity of protein–ligand bonds.

Order	ZINC15 code	Trade name
1	fda_000416	Naldemedine
2	Investigational_only_003715	Maduraphthalazine
3	naturals_000274	Baimantuoluoside B
4	Investigational_only_003469	Merestinib
5	fda_001458	Dasabuvir
6	Investigational_only_000744	Entrectinib
7	Investigational_only_003588	Dersalazine
8	naturals_000004	Withanolide A
9	fda-000728	Risperidone
10	fda_000886	Lumacaftor
11	Investigational_only_001941	Chiglitazar
12	Naturals_000209	Daturafoliside I

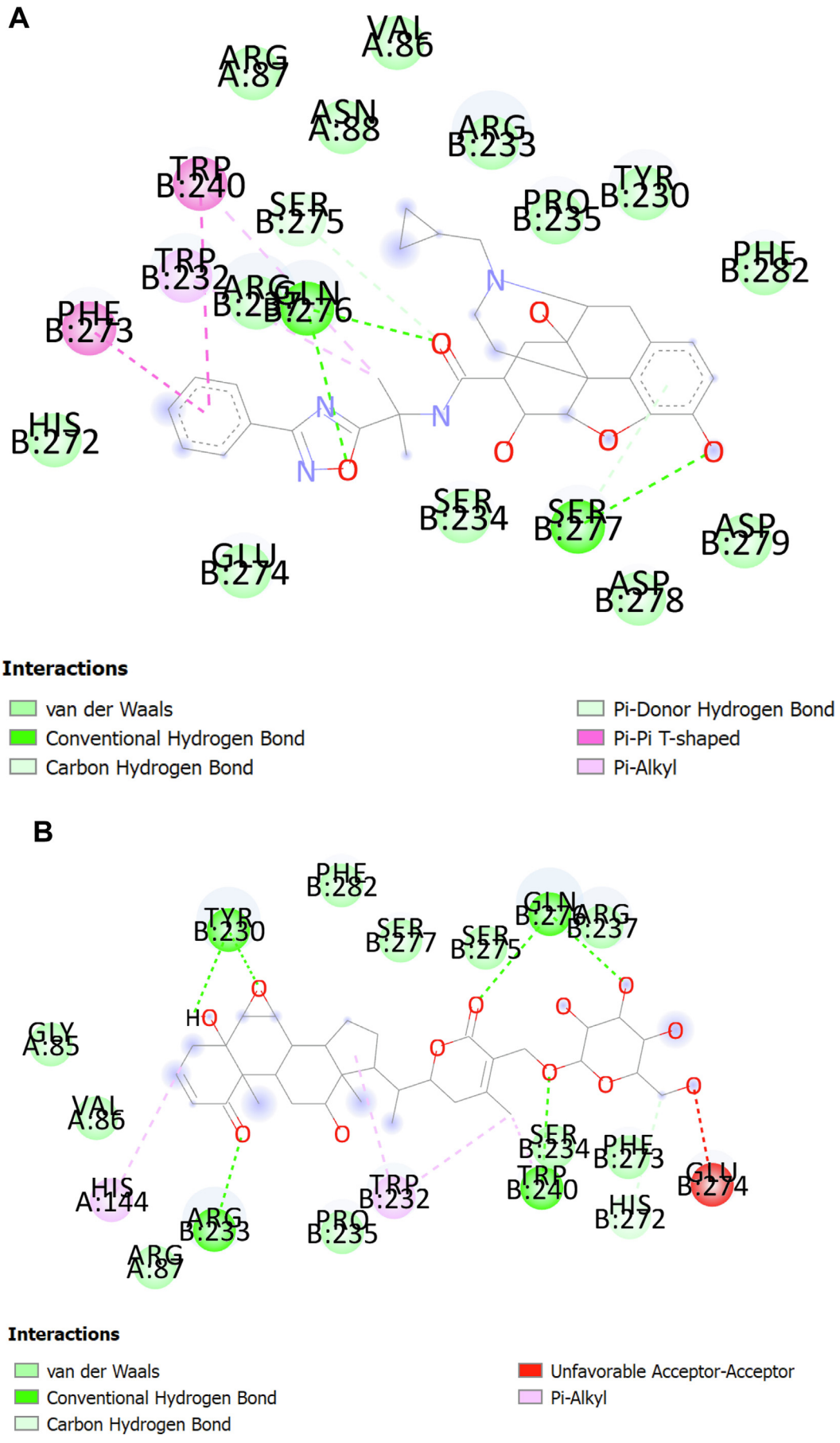

Fig. 1. The interactions of complexes in Discovery studio for A) Naldemedine, B), Baimantuoluoside B, and C) Risperidone.

50 µL, DTT solution 0.5 µL, and caspase substrate 5 µL) was added to the wells and incubated at 4°C for 2 h. A spectrophotometer was used to measure the absorbance of samples at 405 nm. The activity of caspase-7 was calculated according to the formula:

$$Caspase activity(U) = \left(\frac{M \times 105.5}{T} \times 50\right) \times 100$$

M: µM from standard curve plot.
T: Incubated time for each sample in min.

2.10. Expression analysis of caspase-7 using qRT-PCR

Primers were designed using Gene Runner software (Hastings Software, Hudson, NY, USA) and NCBI BLAST tool. The sequences for the forward and reverse primers were designed as CCAAACACTTCTTCATTCAGGCAT, and CTGGAACTGTGGAGTAAGCGA, respectively. The designed primers were synthesized by Copenhagen TAG company (Copenhagen, Denmark) in the lyophilized form. To extract RNA from CHO-K1 cells following treatment with risperidone at several concentrations, RNA isolation kit by RiboEx™ reagent (GeneAll, Korea) was used and the steps were conducted according to the manufacturer's protocol. The concentration and purity of the extracted RNA were confirmed by measurement using a NanoDrop Spectrophotometer (Thermo Fisher Scientific, USA) and agarose gel electrophoresis. For the synthesis of cDNA on the extracted RNA, the FIREScript RT cDNA Synthesis KIT (Solis BioDyne) was employed. Then, caspase-7 mRNA expression was measured by the quantitative reverse transcription polymerase chain reaction (qRT-PCR) using the Roche LightCycler system (Roche, Germany) and the application of RealQ Plus 2x Master Mix Green (Ampliqon, Denmark). The $2^{-\Delta\Delta Ct}$ method was employed for the analysis of caspase-7 relative expression compared to the *GAPDH* gene as an internal control.

3. Results

3.1. Virtual screening

A total number of 450 Iranian herbal compounds in addition to 6,000 chemical compounds including FDA-approved, world-not-FDA approved and investigational compounds, which were retrieved from the ZINC15 database were docked into caspase-7 using PyRx to select those ligands with the highest affinity for amino acids in the active site and binding site of caspase-7. Among them, 100 compounds with the best values were selected and evaluated using Lipinski's rule, which demonstrated 43 ligands with drug-like properties like molecular weight <500 Da, high lipophilicity, having less than 5 hydrogen donor and less than 10 hydrogen acceptors, and molar refraction of 40–130. The number and type of the bonds in the complexes developed between ligand and protein were analyzed by Discovery Studio. The crucial amino acids (Trp232, Phe282, Arg233, Pro235, Gln276, Ser275, Trp240, Asp278, Arg87, Arg237, Leu191, Ser234, His281, Glu284, Trp240, Val86, and Tyr230) of the caspase-7 active site were determined using Uniprot database. Accordingly, the best 12 compounds with the highest number and most potent bonds, including hydrogen bonds, were selected (Table 1). Discovery Studio confirmed the role of these residues in the interaction with those ligands. The interactions in complexes for compounds including Naldemedine, Baimantuoluoside B, and Risperidone are shown in Fig. 1.

3.2. Molecular dynamics

MD simulations of all 12 complexes and unliganded caspase-7 were conducted to screen the compound with the lowest level of free energy (ΔG_{bind}) and the highest stability. The results of the docking score and ΔG_{bind} demonstrated that all screened compounds had good affinities to caspase-7 (Table 2). However, among them, fda-000728 with a ΔG_{bind} of −164,8022143 Kj/mol

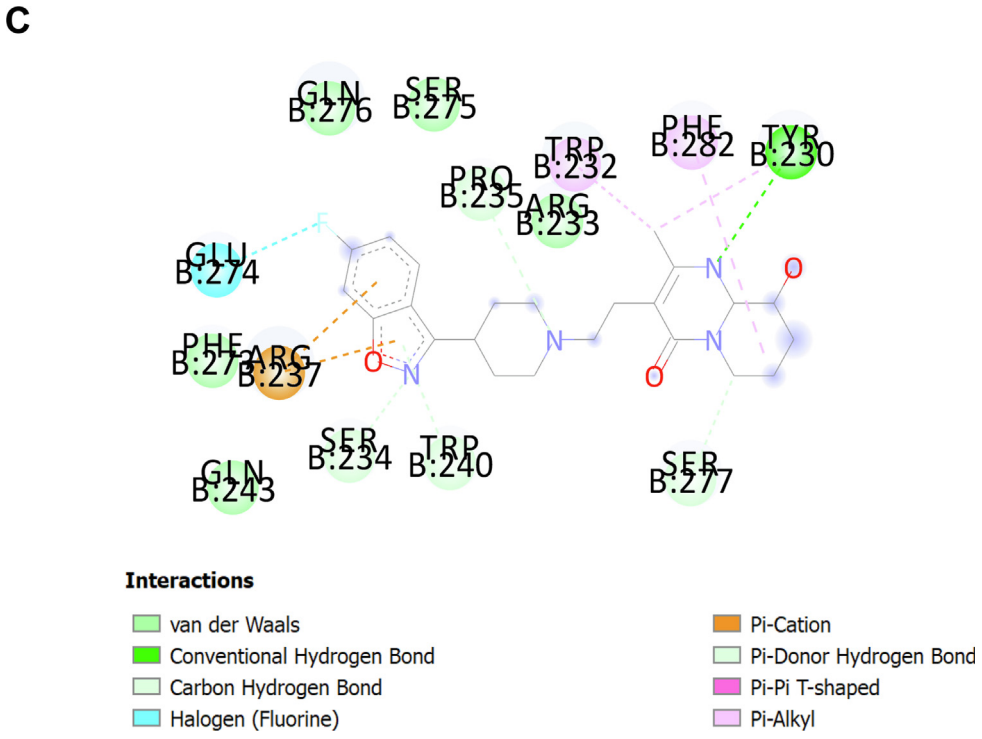

Fig. 1 (*continued*)

Table 2
The MM/PBSA binding free energies of the selected 12 ligands in binding to caspase 7.

Ligand ID	Compound Name	Binding energy (KJ/mol)
Delta_E_binding3715	Maduraphthalazine	−249
Delta_E_binding744	Entrectinib	−238
Delta_E_binding3588	Dersalazine	−234
Delta_E_binding3469	Merestinib	−217
Delta_E_binding-nat274	Baimantuoluoside B	−214
Delta_E_binding-nat4	Withanolide A	−211
Delta_E_binding-nat209	Daturafoliside I	−202
Delta_E_binding1941	Chiglitazar	−185
Delta_E_binding416	Naldemedine	−166
Delta_E_binding886	Lumacaftor	−165
Delta_E_binding728	Risperidone	−164
Delta_E_binding1458	Dasabuvir	−160

that corresponded to risperidone as a conventional antipsychotic drug was selected due to several criteria like accessibility, costs and clinical application. Accordingly, we examined the impact of risperidone on the inhibition of caspase-7 activity and apoptosis.

Fig. 2 illustrates the interaction of risperidone with caspase-7 active site residues.

3.3. Risperidone is a safe treatment for CHO cells

The toxicity of risperidone on CHO cells was evaluated in 100 nM, 20 μM, and 100 μM in 24, 48, and 72 h post-treatment. Since dimethyl sulfoxide (DMSO) solvent was used to dissolve risperidone, we also tested two dilutions of DMSO 1% and 0.5% to check the toxicity of DMSO solvent on cells. The results of the MTT assay revealed that the cytotoxicity of risperidone at all concentrations was lower than 50%, and thus, it can be considered safe for CHO cells (Table 3).

3.4. Risperidone inhibits caspase-7 activity in CHO cells

Since none of risperidone's concentrations demonstrated significant toxicity on CHO cells, its impact on the inhibition of caspase-7 was evaluated at 3 concentrations of 1, 25, and 50 μM. The results revealed that after 24 h of risperidone treatment, the activity of caspase-7 significantly decreased at 1, and 25 mM concentrations, while the inhibition happened at all concentrations of risperidone after 48 and 72 h of treatment (Fig. 3).

3.5. Risperidone inhibits apoptosis of CHO cells

The results of annexin V apoptosis assay following confirmation with flowcytometry revealed that the number of viable cells in risperidone-treated CHO-K1 cells after 24 h significantly increased in the 25 μM concentration of risperidone compared to the control untreated group (increase from a basic level of 88% to 89%), while the increasing change in 1 μM concentration was not significant. Significant enhancement in the viability of CHO-K1 cells was also seen in 1, and 25 μM in two distinct times of 48, and 72 h post-treatment, respectively (Fig. 4).

3.6. Risperidone exerts an anti-apoptotic role through suppression of caspase-7 activity

The results of qRT-PCR demonstrated increased expression of the gene in response to risperidone treatment at three concentrations 48 h post-treatment relative to *GAPDH* treatment. It seems risperidone does not have any impact on caspase-7 expression; however, since it is suggested that risperidone inhibits caspase-7, negative feedback develops within the treated cells to compensate for the risperidone-mediated caspase-7 inhibition (Fig. 5). These data demonstrated that risperidone showed an anti-apoptotic role in CHO cells through inhibition of caspase-7 and thus, may prolong

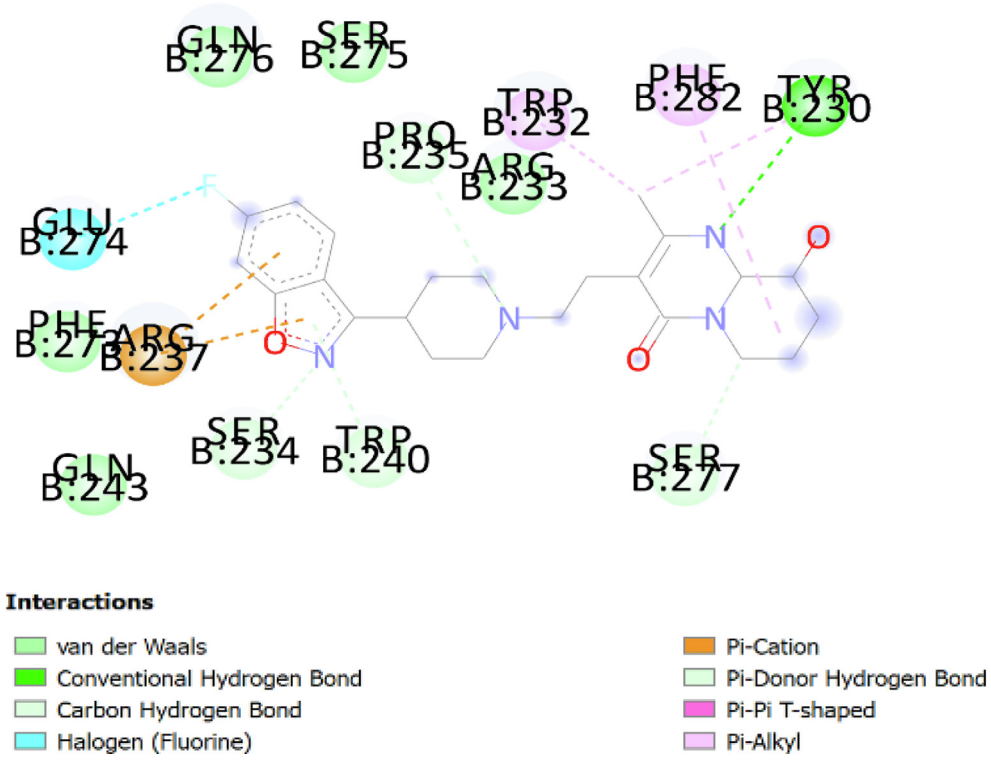

Fig. 2. The interaction between risperidone and residues in caspase-7 illustrated by PyMOL.

Table 3
The results of risperidone's toxicity evaluation on CHO cells in the MTT assay in 24, 48, and 72 h post-treatment.

24 h post-treatment						
Concentration	100 µM	20 µM	100 nM	Control	DMSO 1%	DMSO 0.5%
Optical density (OD)	0.124	0.205	0.184	0.224	0.179	0.196
Cytotoxicity%	44.6	8.4	17.8	0.0	20	12.5
Viability %	55.4	91.6	82.2	100	80	87.5
48 h post-treatment						
Concentration	100 µM	20 µM	100 nM	Control	DMSO 1%	DMSO 0.5%
OD	0.363	0.566	0.66	0.796	0.383	0.42
Cytotoxicity%	54.3	28.8	17.08	0.0	51.8	47.2
Viability %	45.7	71.2	82.92	100	48.2	52.8
72 h post-treatment						
Concentration	100 µM	20 µM	100 nM	Control	DMSO 1%	DMSO 0.5%
OD	0.359	0.716	0.875	0.803	0.380	0.43
Cytotoxicity%	55.2	10.83	–	0.0	52.67	48.5
Viability %	44.8	89.17	100	100	47.33	51.5

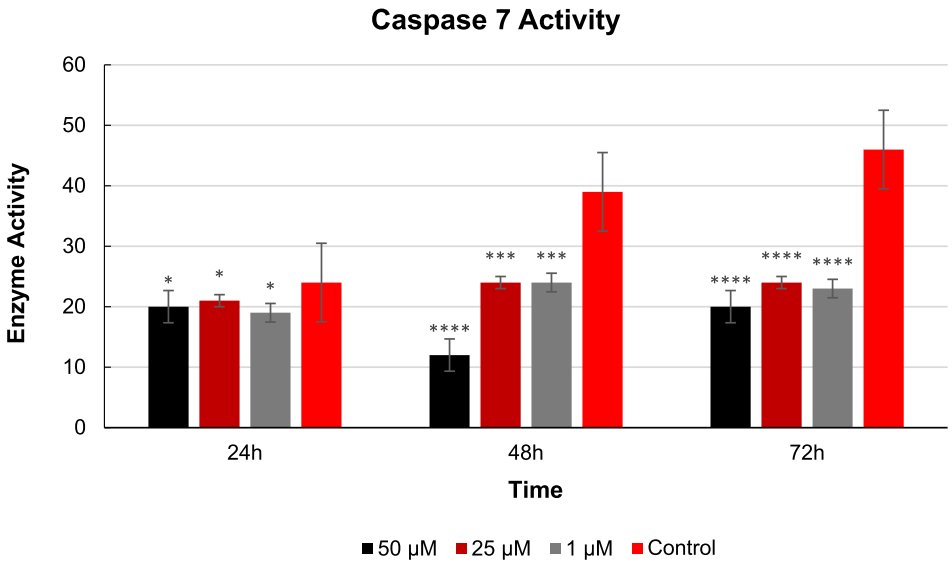

Fig. 3. The impact of risperidone on the inhibition of caspase-7 activity. The results are demonstrated as caspase-7 activity ± SD in treatment groups compared to control. * Equals $p \leq 0.05$, ** showing $p \leq 0.01$, *** representing $p \leq 0.001$, and **** for $p \leq 0.0001$.

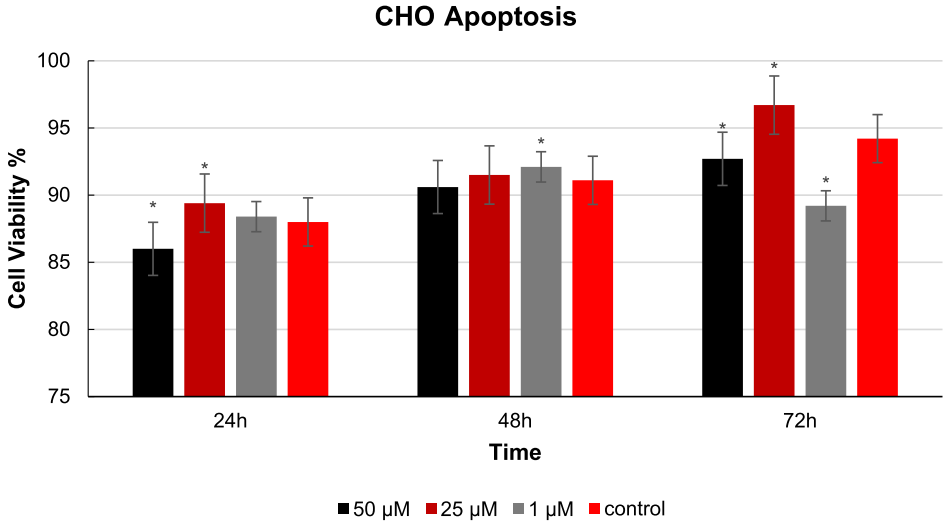

Fig. 4. The impact of risperidone treatment on the apoptosis and viability of CHO cells. The results are demonstrated as caspase-7 activity ± SD in treatment groups compared to control. * Equals $p \leq 0.05$.

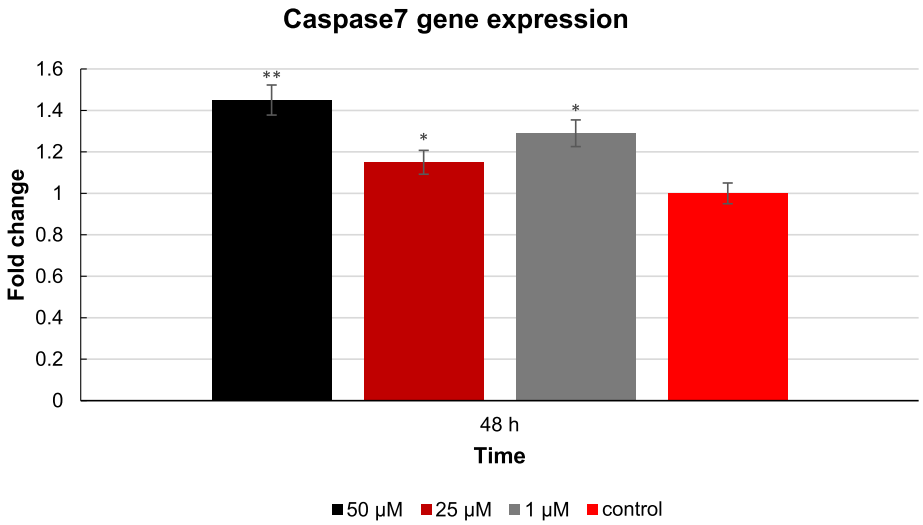

Fig. 5. The expression of caspase 7 in response to risperidone treatment in qRT-PCR. The values are presented as ± SD. * Equals $p \leq 0.05$, and ** represents $p \leq 0.01$.

the lifespan of these cells with applications in biotechnology and industry.

4. Discussion

CHO cells are the most used eukaryotic cells for the large-scale production of recombinant therapeutic proteins [29]. Some significant advances have been achieved in the applicability and protein yield of CHO cells during the past decades. The productivity of CHO cells, for instance, has been improved by more than 9-fold from 10 pg/cell/day in 1986 to 90 pg/cells/day in the early 21st century [30]. Theoretically, prolonging the survival of CHO cells through inhibition of apoptosis may enable us to enhance their productivity. Caspase-7 is an executioner caspase, which plays substantial roles in the programmed cell death and regulating cell survival. In this study, we screened several native Iranian herbal compounds, which potentially inhibited caspase-7. Findings of virtual screening and molecular dynamics suggested risperidone to target caspase-7. Toxicity evaluation using MTT assessment confirmed the safety of risperidone on CHO cells, while its treatment inhibited caspase-7 activity. Annexin V apoptosis assay also revealed that risperidone may improve the viability of CHO cells. Overall, this study suggested that caspase-7 inhibition using risperidone may act as an approach to enhance the survival and consequently productivity of CHO cells. Risperidone is an antipsychotic drug, for which some studies already report a controversial impact on the apoptosis of various cells [31,32]. Further studies are recommended to confirm the applicability of risperidone for enhancing the survival of CHO cells and consequently potential improvement of applicability.

Financial support

This study was supported by Shahid Beheshti University of Medical Sciences (Grant No: 43003045/ IR.SBMU.RETECH.REC.1401.887).

Conflict of interest

The authors have no conflicts of interest to declare.

CRediT authorship contribution statement

Sara Kafi: Methodology. **Sajad Najafi:** Methodology, Writing – original draft, Writing – review & editing. **Karim Mahnam:** Methodology, Data curation, Formal analysis. **Shirin Farivar:** Conceptualization, Methodology, Writing – review & editing, Data curation, Formal analysis. **Javad Ranjbari:** Conceptualization, Data curation, Methodology, Software, Supervision, Validation, Writing – original draft, Writing – review & editing.

Supplementary material

https://doi.org/10.1016/j.ejbt.2024.04.007.

Data availability

The data that support the findings of this study are available from the corresponding author (JR) upon reasonable request.

References

[1] Pham PV. Medical Biotechnology: Techniques and Applications. In: Barh D, Azevedo V, editors. Omics Technologies and Bio-Engineering. Academic Press; 2018. p. 449-469. https://doi.org/10.1016/B978-0-12-804659-3.00019-1 PMid: 29193228.
[2] Lagassé HAD, Alexaki A, Simhadri VL, et al. Recent advances in (therapeutic protein) drug development. F1000Res 2017;6:113. https://doi.org/10.12688/f1000research.9970.1. PMid: 28232867.
[3] Gupta V, Sengupta M, Prakash J, et al. Production of recombinant pharmaceutical proteins. In: Gupta V, Sengupta M, Prakash J, editors. Basic and Applied Aspects of Biotechnology. Singapore: Springer Singapore; 2017. p. 77–101. https://doi.org/10.1007/978-981-10-0875-7_4.
[4] Nosaki S, Miura K. Transient expression of recombinant proteins in plants. Methods Enzymol 2021;660:193–203. https://doi.org/10.1016/bs.mie.2021.04.021. PMid: 34742388.
[5] Gupta SK, Shukla P. Sophisticated cloning, fermentation, and purification technologies for an enhanced therapeutic protein production: A review. Front Pharmacol 2017;8:419. https://doi.org/10.3389/fphar.2017.00419. PMid: 28725194.
[6] Dahodwala H, Lee KH. The fickle CHO: A review of the causes, implications, and potential alleviation of the CHO cell line instability problem. Curr Opin Biotechnol 2019;60:128–37. https://doi.org/10.1016/j.copbio.2019.01.011. PMid: 30826670.
[7] Reinhart D, Damjanovic L, Kaisermayer C, et al. Bioprocessing of recombinant CHO-K1, CHO-DG44, and CHO-S: CHO expression hosts favor either mAb production or biomass synthesis. Biotechnol J 2019;14(3):e1700686. https://doi.org/10.1002/biot.201700686. PMid: 29701329.
[8] Vieira HL, Pereira AC, Peixoto CC, et al. Improvement of recombinant protein production by an anti-apoptotic protein from hemolymph of *Lonomia obliqua*.

Cytotechnology 2010;62(6):547–55. https://doi.org/10.1007/s10616-010-9305-x. PMid: 20936342.
[9] Van Opdenbosch N, Lamkanfi M. Caspases in cell death, inflammation, and disease. Immunity 2019;50(6):1352–64. https://doi.org/10.1016/j.immuni.2019.05.020. PMid: 31216460.
[10] Julien O, Wells JA. Caspases and their substrates. Cell Death Differ 2017;24(8):1380–9. https://doi.org/10.1038/cdd.2017.44. PMid: 28498362.
[11] Jan R, Chaudhry GE. Understanding apoptosis and apoptotic pathways targeted cancer therapeutics. Adv Pharm Bull 2019;9(2):205–18. PMid: 31380246.
[12] Lamkanfi M, Kanneganti TD. Caspase-7: A protease involved in apoptosis and inflammation. Int J Biochem Cell Biol 2010;42(1):21–4. https://doi.org/10.1016/j.biocel.2009.09.013. PMid: 19782763.
[13] Najafi S, Alibakhshi A, Mahnam K, et al. Docking study on Caspase 3 inhibitors as potential drugs for traumatic brain cell apoptosis. Lett Drug Des Discov 2024;21(3):542–51. https://doi.org/10.2174/1570180819666220915101829.
[14] Pham B, Eron SJ, Hill ME, et al. A nanopore approach for analysis of Caspase-7 activity in cell lysates. Biophys J 2019;117(5):844–55. https://doi.org/10.1016/j.bpj.2019.07.045. PMid: 31427065.
[15] Parui AL, Bose K. Caspases: Regulatory mechanisms and their implications in pathogenesis and therapeutics. In: Chakraborti S, Dhalla NS, editors. Pathophysiological Aspects of Proteases. Singapore: Springer Singapore; 2017. p. 423–88. https://doi.org/10.1007/978-981-10-6141-7_18.
[16] Chai J, Wu Q, Shiozaki E, et al. Crystal structure of a procaspase-7 zymogen: Mechanisms of activation and substrate binding. Cell 2001;107(3):399–407. https://doi.org/10.1016/S0092-8674(01)00544-X. PMid: 11701129.
[17] Sterling T, Irwin JJ. ZINC 15 -Ligand discovery for everyone. J Chem Inf Model 2015;55(11):2324–37. https://doi.org/10.1021/acs.jcim.5b00559. PMid: 26479676.
[18] Pettersen EF, Goddard TD, Huang CC, et al. UCSF Chimera -A visualization system for exploratory research and analysis. J Comput Chem 2004;25(13):1605–12. https://doi.org/10.1002/jcc.20084. PMid: 15264254.
[19] O'Boyle NM, Banck M, James CA, et al. Open Babel: An open chemical toolbox. J Cheminform 2011;3:33. https://doi.org/10.1186/1758-2946-3-33. PMid: 21982300.
[20] Forli S, Huey R, Pique ME, et al. Computational protein-ligand docking and virtual drug screening with the AutoDock suite. Nat Protoc 2016;11(5):905–19. https://doi.org/10.1038/nprot.2016.051. PMid: 27077332.
[21] Dallakyan S, Olson AJ. Small-molecule library screening by docking with PyRx. Methods Mol Biol 2015;1263:243–50. https://doi.org/10.1007/978-1-4939-2269-7_19. PMid: 25618350.
[22] Schrodinger L. The PyMOL molecular graphics system. Version. 1.3r1. 2010.
[23] Dassault Systèmes BIOVIA, Discovery Studio Modeling Environment, Release 2017, San Diego: Dassault Systèmes, 2016.
[24] Cheng F, Li W, Zhou Y, et al. admetSAR: A comprehensive source and free tool for assessment of chemical ADMET properties. J Chem Inf Model 2012;52(11):3099–105. https://doi.org/10.1021/ci300367a. PMid: 23092397.
[25] Daina A, Michielin O, Zoete V. SwissADME: A free web tool to evaluate pharmacokinetics, drug-likeness and medicinal chemistry friendliness of small molecules. Sci Rep 2017;7:42717. https://doi.org/10.1038/srep42717. PMid: 28256516.
[26] Barkhordari A, Mahnam K, Mirmohammad-Sadeghi H. Designing a new bispecific tandem single-chain variable fragment antibody against tumor necrosis factor-α and interleukin-23 using in silico studies for the treatment of rheumatoid arthritis. J Mol Model 2020;26(9):225. https://doi.org/10.1007/s00894-020-04510-5. PMid: 32778954.
[27] Kumari R, Kumar R.Open Source Drug Discovery Consortium, et al. *g_mmpbsa* - A GROMACS tool for high-throughput MM-PBSA calculations. J Chem Inf Model 2014;54(7):1951–62. https://doi.org/10.1021/ci500020m. PMid: 24850022.
[28] Genheden S, Ryde U. The MM/PBSA and MM/GBSA methods to estimate ligand-binding affinities. Expert Opin Drug Discov 2015;10(5):449–61. https://doi.org/10.1517/17460441.2015.1032936. PMid: 25835573.
[29] Yamaguchi K, Ogawa R, Tsukahara M, et al. Efficient production of recombinant proteins in suspension CHO cells culture using the *Tol2* transposon system coupled with cycloheximide resistance selection. Sci Rep 2023;13(1):7628. https://doi.org/10.1038/s41598-023-34636-4. PMid: 37165015.
[30] Szkodny AC, Lee KH. Biopharmaceutical manufacturing: Historical perspectives and future directions. Annu Rev Chem Biomol Eng 2022;13:141–65. https://doi.org/10.1146/annurev-chembioeng-092220-125832. PMid: 35300518.
[31] Zheng L, Yang L, Zhao X, et al. Effect of risperidone on proliferation and apoptosis of MC3T3-E1 cells. Braz J Med Biol Res 2019;52(3):e8098. https://doi.org/10.1590/1414-431x20188098. PMid: 30810624.
[32] Pang L, Li P, Zheng L, et al. Risperidone induces apoptosis of human osteoblast cell line hFob1.19 through Wnt/β-catenin signaling pathway. Basic. Clin Med 2023;43(3):374–9. https://doi.org/10.16352/j.issn.1001-6325.2023.03.374.